

Buckling of Elastic Circular Plate with Surface Stresses



Denis N. Sheydakov

Abstract In the framework of general stability theory for three-dimensional bodies, the buckling analysis has been carried out for a circular plate subjected to the radial compression. It was assumed that the surface stresses are acting on its faces and the behavior of the plate is described by the Gurtin–Murdoch model. For an arbitrary isotropic material, the system of linearized equilibrium equations is derived, which describes the behavior of a plate in a perturbed state. In the case of axisymmetric perturbations, the stability analysis is reduced to solving a linear homogeneous boundary-value problem for a system of three ordinary differential equations. It is shown that for a plate with identical faces, it is sufficient to consider only half of the plate to study its stability. For two specific models of bulk material (Harmonic model and Blatz–Ko model), the buckling analysis has been carried out for a circular plate made of aluminum. It was found, in particular, that the stability of the plate increases with a decrease in its overall size. This effect is due to the influence of surface stresses and is quite significant at the micro- and nanoscale.

1 Introduction

The problem of equilibrium stability for deformable bodies is of major importance because the exhaustion of bearing capacity and the collapse of engineering structures quite often occurs due to the buckling under external loads. Due to the development of modern technologies and the appearance of new materials, the problem of stability analysis while taking into account the various surface phenomena becomes relevant [11]. For example, the deformation pattern of bodies at micro- and nanoscale is often significantly different from the behavior of macro-sized bodies, which can be explained by surface effects [1]. To model surface phenomena, especially in nanomechanics [4, 17], the theory of elasticity with surface stresses has received development. In this theory, in addition to the ordinary stresses distributed in the

D. N. Sheydakov (✉)
South Scientific Center of Russian Academy of Sciences, Chekhova Ave. 41,
344006 Rostov-on-Don, Russia
e-mail: sheidakov@mail.ru

volume, the independent surface stresses are also taken into account at the boundary of the body or its part. These stresses generalize the well-known in hydromechanics scalar surface tension to the case of solids. The introduction of surface stresses allows, in particular, describing the size effect typical for nanomaterials [3, 9, 16].

The present research is dedicated to the buckling analysis of nonlinearly elastic plates with surface stresses. To take into account the influence of the latter, the Gurtin–Murdoch model [6] is used, which from the mechanical point of view is equivalent to a deformable body with a glued elastic membrane. Accounting for surface stresses allows studying the buckling features of micro- and nanosized plates.

2 Governing Equations

In the framework of Gurtin–Murdoch model, the set of static equations for a nonlinearly elastic body with surface stresses in the absence of body forces consists of [14] the equilibrium equations

$$\overset{\circ}{\nabla} \cdot \mathbf{D} = \mathbf{0} \tag{1}$$

the equilibrium conditions on the part of the body surface Ω_s , where the surface stresses are acting

$$\left(\mathbf{n} \cdot \mathbf{D} - \overset{\circ}{\nabla}_s \cdot \mathbf{D}_s \right) \Big|_{\Omega_s} = \mathbf{t} \tag{2}$$

the constitutive equations

$$\mathbf{D} = \mathbf{P} \cdot \mathbf{C}, \quad \mathbf{P} = 2 \frac{\partial W(\mathbf{G})}{\partial \mathbf{G}}, \quad \mathbf{D}_s = \mathbf{P}_s \cdot \mathbf{C}_s, \quad \mathbf{P}_s = 2 \frac{\partial W_s(\mathbf{G}_s)}{\partial \mathbf{G}_s} \tag{3}$$

and the geometric relations

$$\mathbf{G} = \mathbf{C} \cdot \mathbf{C}^T, \quad \mathbf{C} = \overset{\circ}{\nabla} \mathbf{R}, \quad \mathbf{G}_s = \mathbf{C}_s \cdot \mathbf{C}_s^T, \quad \mathbf{C}_s = \overset{\circ}{\nabla}_s \mathbf{R} \Big|_{\Omega_s} \tag{4}$$

Here \mathbf{D} and \mathbf{P} are the Piola and Kirchhoff stress tensors, respectively; $\overset{\circ}{\nabla}$ is the three-dimensional nabla-operator in Lagrangian coordinates; $\overset{\circ}{\nabla}_s$ is the surface nabla-operator; \mathbf{D}_s and \mathbf{P}_s are the surface stress tensors of the Piola and Kirchhoff type; \mathbf{n} is the unit vector normal to the surface of the undeformed body; \mathbf{t} is the surface loads vector; W and W_s are the bulk and surface strain energy densities, respectively; \mathbf{G} and \mathbf{G}_s are the Cauchy–Green strain tensors in the volume and on the surface of the body; \mathbf{C} and \mathbf{C}_s are the deformation gradients; and \mathbf{R} is the position vector in the actual configuration.

Taking (3) into account, the following relations are valid for the Kirchhoff stress tensor \mathbf{P} in the case of an isotropic body [8, 10]:

$$\mathbf{P} = \sum_{k=1}^3 \chi_k \mathbf{d}_k \otimes \mathbf{d}_k, \quad \chi_k = 2 \frac{\partial W(G_1, G_2, G_3)}{\partial G_k}, \quad \mathbf{G} = \sum_{k=1}^3 G_k \mathbf{d}_k \otimes \mathbf{d}_k \quad (5)$$

where $G_k, \mathbf{d}_k (k = 1, 2, 3)$ are the eigenvalues and eigenvectors of the Cauchy–Green strain tensor \mathbf{G} . At the same time, the expression for the surface stress tensor of Kirchhoff type \mathbf{P}_s takes the form [1]:

$$\mathbf{P}_s = \kappa_1 \mathbf{I}_s + 2\kappa_2 \mathbf{G}_s, \quad \kappa_\theta = 2 \frac{\partial W_s(j_1, j_2)}{\partial j_\theta}, \quad j_\theta = \text{tr} \mathbf{G}_s^\theta, \quad \theta = 1, 2 \quad (6)$$

Here j_1, j_2 are the invariants of the surface Cauchy–Green strain tensor \mathbf{G}_s ; \mathbf{I} and $\mathbf{I}_s = \mathbf{I} - \mathbf{n} \otimes \mathbf{n}$ are the three-dimensional and surface unit tensors, respectively.

3 Circular Plate with Surface Stresses

Consider a homogeneous circular plate of radius r_0 and thickness $2h$. We assume that the surface stresses are acting on its top Ω_+ ($z = h$) and bottom Ω_- ($z = -h$) faces, i.e. $\Omega_s = \Omega_+ \cup \Omega_-$. In the case of radial compression of the plate, the position vector \mathbf{R} is given by the following relations [13, 18]:

$$\begin{aligned} \mathbf{R} &= \alpha r \mathbf{e}_R + \gamma z \mathbf{e}_Z \\ R &= \alpha r, \quad \Phi = \varphi, \quad Z = \gamma z \\ 0 \leq r \leq r_0, \quad 0 \leq \varphi \leq 2\pi, \quad |z| \leq h \end{aligned} \quad (7)$$

where r, φ, z are the cylindrical coordinates in the reference state (Lagrangian coordinates); R, Φ, Z are the Eulerian cylindrical coordinates; $\{\mathbf{e}_r, \mathbf{e}_\varphi, \mathbf{e}_z\}$ and $\{\mathbf{e}_R, \mathbf{e}_\Phi, \mathbf{e}_Z\}$ are the orthonormal vector bases of Lagrangian and Eulerian coordinates, respectively; α is the given ratio of radial compression; and γ is the unknown constant that characterizes the deformation in the thickness direction of the plate.

According to the expressions (4), (7), the deformation gradients in the volume and on the surface are:

$$\mathbf{C} = \alpha(\mathbf{e}_r \otimes \mathbf{e}_R + \mathbf{e}_\varphi \otimes \mathbf{e}_\Phi) + \gamma \mathbf{e}_z \otimes \mathbf{e}_Z, \quad \mathbf{C}_\pm = \alpha(\mathbf{e}_r \otimes \mathbf{e}_R + \mathbf{e}_\varphi \otimes \mathbf{e}_\Phi) \quad (8)$$

Hereinafter indexes “+” and “-” denote surface quantities related to the top and bottom faces of the circular plate, respectively.

From the relations (4), (8) we obtain the expressions for the corresponding Cauchy–Green strain tensors

$$\mathbf{G} = \alpha^2(\mathbf{e}_r \otimes \mathbf{e}_r + \mathbf{e}_\varphi \otimes \mathbf{e}_\varphi) + \gamma^2 \mathbf{e}_z \otimes \mathbf{e}_z, \quad \mathbf{G}_\pm = \alpha^2(\mathbf{e}_r \otimes \mathbf{e}_r + \mathbf{e}_\varphi \otimes \mathbf{e}_\varphi) \quad (9)$$

It is obvious that for the considered initial strain state the eigenvectors \mathbf{d}_k ($k = 1, 2, 3$) of the Cauchy–Green strain tensor coincide with the vector basis of Lagrangian cylindrical coordinates, i.e. $\mathbf{d}_1 = \mathbf{e}_r$, $\mathbf{d}_2 = \mathbf{e}_\varphi$, $\mathbf{d}_3 = \mathbf{e}_z$, and the eigenvalues G_k are: $G_1 = G_2 = \alpha^2$, $G_3 = \gamma^2$. Thus, taking (5), (6) into account, the following relations are valid for the Kirchhoff stress tensors:

$$\begin{aligned} \mathbf{P} &= \chi_1 \mathbf{e}_r \otimes \mathbf{e}_r + \chi_2 \mathbf{e}_\varphi \otimes \mathbf{e}_\varphi + \chi_3 \mathbf{e}_z \otimes \mathbf{e}_z \\ \mathbf{P}_\pm &= (\kappa_1^\pm + 2\alpha^2 \kappa_2^\pm) (\mathbf{e}_r \otimes \mathbf{e}_r + \mathbf{e}_\varphi \otimes \mathbf{e}_\varphi) \end{aligned} \quad (10)$$

Substituting the above expressions in (3), we find a representation of the Piola stress tensor \mathbf{D} and the surface stress tensors of the Piola type \mathbf{D}_+ and \mathbf{D}_- in the case of radial compression of the circular plate

$$\begin{aligned} \mathbf{D} &= \alpha \chi_1 \mathbf{e}_r \otimes \mathbf{e}_r + \alpha \chi_2 \mathbf{e}_\varphi \otimes \mathbf{e}_\varphi + \gamma \chi_3 \mathbf{e}_z \otimes \mathbf{e}_z \\ \mathbf{D}_\pm &= \alpha (\kappa_1^\pm + 2\alpha^2 \kappa_2^\pm) (\mathbf{e}_r \otimes \mathbf{e}_r + \mathbf{e}_\varphi \otimes \mathbf{e}_\varphi) \end{aligned} \quad (11)$$

It follows from (11) that the equilibrium equations (1) are automatically satisfied if $\chi_1 = \chi_2$. The equilibrium conditions (2) on the plate faces Ω_+ and Ω_- in the absence of surface loads are written as follows:

$$\chi_3|_{z=\pm h} = 0 \quad (12)$$

By solving the equation (12) at given density W of the bulk strain energy, we find the unknown constant γ .

4 Equations of Neutral Equilibrium

Suppose that in addition to the discussed initial strain state of the circular plate with surface stresses, there is an infinitely close equilibrium state under the same external loads, which is determined by the position vector $\tilde{\mathbf{R}} = \mathbf{R} + \eta \mathbf{v}$. Here η is the small parameter and \mathbf{v} is the vector of additional displacements.

The linearized equilibrium equations for a nonlinearly elastic medium have the form [5, 10]:

$$\overset{\circ}{\nabla} \cdot \mathbf{D}^\bullet = \mathbf{0}, \quad \mathbf{D}^\bullet = \left[\frac{d}{d\eta} \mathbf{D}(\mathbf{R} + \eta \mathbf{v}) \right]_{\eta=0} \quad (13)$$

$$\mathbf{D}^\bullet = \mathbf{P}^\bullet \cdot \mathbf{C} + \mathbf{P} \cdot \overset{\circ}{\nabla} \mathbf{v} \quad (14)$$

Here \mathbf{D}^\bullet and \mathbf{P}^\bullet are the linearized Piola and Kirchhoff stress tensors, respectively. In order to find the expression for the latter, a linearization of the constitutive relations (5) is carried out [12, 14]

$$\begin{aligned}
 \mathbf{P}^\bullet &= \sum_{k=1}^3 (\chi_k^\bullet \mathbf{d}_k \otimes \mathbf{d}_k + \chi_k \mathbf{d}_k^\bullet \otimes \mathbf{d}_k + \chi_k \mathbf{d}_k \otimes \mathbf{d}_k^\bullet) \\
 \mathbf{G}^\bullet &= \sum_{k=1}^3 (G_k^\bullet \mathbf{d}_k \otimes \mathbf{d}_k + G_k \mathbf{d}_k^\bullet \otimes \mathbf{d}_k + G_k \mathbf{d}_k \otimes \mathbf{d}_k^\bullet)
 \end{aligned}
 \tag{15}$$

By taking into account the fact that vectors \mathbf{d}_k and \mathbf{d}_k^\bullet ($k = 1, 2, 3$) are mutually orthogonal, i.e. $\mathbf{d}_k \cdot \mathbf{d}_k^\bullet = 0$, following (15) we obtain ($m, n = 1, 2, 3; k \neq m \neq n$)

$$\mathbf{d}_k \cdot \mathbf{P}^\bullet \cdot \mathbf{d}_k = \chi_k^\bullet, \quad \mathbf{d}_k \cdot \mathbf{P}^\bullet \cdot \mathbf{d}_m = B_n \mathbf{d}_k \cdot \mathbf{G}^\bullet \cdot \mathbf{d}_m, \quad B_n = \frac{\chi_k - \chi_m}{G_k - G_m}
 \tag{16}$$

where the relations for χ_k^\bullet have the form:

$$\chi_k^\bullet = \sum_{n=1}^3 \chi_{kn} G_n^\bullet, \quad \chi_{kn} = \frac{\partial \chi_k(G_1, G_2, G_3)}{\partial G_n}, \quad G_n^\bullet = \mathbf{d}_n \cdot \mathbf{G}^\bullet \cdot \mathbf{d}_n$$

Equations (16) represent all components of the linearized Kirchhoff stress tensor \mathbf{P}^\bullet in the basis $\{\mathbf{d}_1, \mathbf{d}_2, \mathbf{d}_3\}$ through the components of the linearized Cauchy–Green strain tensor \mathbf{G}^\bullet , while the tensor \mathbf{G}^\bullet itself is

$$\mathbf{G}^\bullet = \overset{\circ}{\nabla} \mathbf{v} \cdot \mathbf{C}^T + \mathbf{C} \cdot \overset{\circ}{\nabla} \mathbf{v}^T
 \tag{17}$$

According to (2), the linearized equilibrium conditions on the top ($z = h$) and bottom ($z = -h$) faces of the plate take the form [1]:

$$\left(\mathbf{e}_z \cdot \mathbf{D}^\bullet \mp \overset{\circ}{\nabla}_\pm \cdot \mathbf{D}_\pm^\bullet \right) \Big|_{z=\pm h} = \mathbf{0}
 \tag{18}$$

Here \mathbf{D}_+^\bullet and \mathbf{D}_-^\bullet are the linearized surface stress tensors of the Piola type, for which, taking into account the expressions (3), (6), the following relations are valid [15]

$$\mathbf{D}_\pm^\bullet = \mathbf{P}_\pm^\bullet \cdot \mathbf{C}_\pm + \mathbf{P}_\pm \cdot \overset{\circ}{\nabla}_\pm \mathbf{v}_\pm, \quad \mathbf{P}_\pm^\bullet = \kappa_1^\pm \mathbf{I}_\pm + 2\kappa_2^\pm \mathbf{G}_\pm + 2\kappa_2^\pm \mathbf{G}_\pm^\bullet
 \tag{19}$$

where ($\theta = 1, 2$)

$$\begin{aligned}
 \kappa_\theta^\pm &= \sum_{\tau=1}^2 \kappa_{\theta\tau}^\pm j_\tau^\pm, \quad \kappa_{\theta\tau}^\pm = \frac{\partial \kappa_\theta^\pm(j_1^\pm, j_2^\pm)}{\partial j_\tau^\pm} \\
 j_1^\pm &= \text{tr} \mathbf{G}_\pm^\bullet, \quad j_2^\pm = 2 \text{tr} (\mathbf{G}_\pm \cdot \mathbf{G}_\pm^\bullet) \\
 \mathbf{G}_\pm^\bullet &= \overset{\circ}{\nabla}_\pm \mathbf{v}_\pm \cdot \mathbf{C}_\pm^T + \mathbf{C}_\pm \cdot \overset{\circ}{\nabla}_\pm \mathbf{v}_\pm^T, \quad \mathbf{v}_\pm = \mathbf{v} \Big|_{z=\pm h}
 \end{aligned}
 \tag{20}$$

Here \mathbf{P}_+^\bullet and \mathbf{P}_-^\bullet are the linearized surface stress tensors of the Kirchhoff type; \mathbf{G}_+^\bullet and \mathbf{G}_-^\bullet are the linearized surface strain tensors of the Cauchy-Green type; \mathbf{v}_+ and \mathbf{v}_- are the vectors of additional displacements of the plate faces.

We assume that the constant radial displacement is given at the edge of the circular plate ($r = r_0$), the azimuthal displacement is absent, and there is no friction during vertical displacement. This leads to the following linearized edge conditions [13]:

$$\mathbf{e}_r \cdot \mathbf{D}^\bullet \cdot \mathbf{e}_Z|_{r=r_0} = \mathbf{v} \cdot \mathbf{e}_R|_{r=r_0} = \mathbf{v} \cdot \mathbf{e}_\phi|_{r=r_0} = 0 \quad (21)$$

The vector of additional displacements \mathbf{v} in the basis of Eulerian cylindrical coordinates is written as:

$$\mathbf{v} = v_R \mathbf{e}_R + v_\phi \mathbf{e}_\phi + v_Z \mathbf{e}_Z \quad (22)$$

Taking into account the expressions (8), (10), (14), (16), (17), (22) and the fact that in the considered unperturbed state $\mathbf{d}_1 = \mathbf{e}_r$, $\mathbf{d}_2 = \mathbf{e}_\phi$, $\mathbf{d}_3 = \mathbf{e}_z$, the components of the linearized Piola stress tensor \mathbf{D}^\bullet in the basis of cylindrical coordinates take the form:

$$\begin{aligned} \mathbf{e}_r \cdot \mathbf{D}^\bullet \cdot \mathbf{e}_R &= (\chi_1 + 2\alpha^2 \chi_{11}) \frac{\partial v_R}{\partial r} + \frac{2\alpha^2 \chi_{12}}{r} \left(\frac{\partial v_\phi}{\partial \varphi} + v_R \right) + 2\alpha\gamma \chi_{13} \frac{\partial v_Z}{\partial z} \\ \mathbf{e}_r \cdot \mathbf{D}^\bullet \cdot \mathbf{e}_\phi &= (\chi_1 + \alpha^2 B_3) \frac{\partial v_\phi}{\partial r} + \frac{\alpha^2 B_3}{r} \left(\frac{\partial v_R}{\partial \varphi} - v_\phi \right) \\ \mathbf{e}_r \cdot \mathbf{D}^\bullet \cdot \mathbf{e}_Z &= (\chi_1 + \gamma^2 B_2) \frac{\partial v_Z}{\partial r} + \alpha\gamma B_2 \frac{\partial v_R}{\partial z} \\ \mathbf{e}_\phi \cdot \mathbf{D}^\bullet \cdot \mathbf{e}_R &= \alpha^2 B_3 \frac{\partial v_\phi}{\partial r} + \frac{\chi_2 + \alpha^2 B_3}{r} \left(\frac{\partial v_R}{\partial \varphi} - v_\phi \right) \\ \mathbf{e}_\phi \cdot \mathbf{D}^\bullet \cdot \mathbf{e}_\phi &= 2\alpha^2 \chi_{12} \frac{\partial v_R}{\partial r} + \frac{\chi_2 + 2\alpha^2 \chi_{22}}{r} \left(\frac{\partial v_\phi}{\partial \varphi} + v_R \right) + 2\alpha\gamma \chi_{23} \frac{\partial v_Z}{\partial z} \\ \mathbf{e}_\phi \cdot \mathbf{D}^\bullet \cdot \mathbf{e}_Z &= \frac{\chi_2 + \gamma^2 B_1}{r} \frac{\partial v_Z}{\partial \varphi} + \alpha\gamma B_1 \frac{\partial v_\phi}{\partial z} \\ \mathbf{e}_z \cdot \mathbf{D}^\bullet \cdot \mathbf{e}_R &= (\chi_3 + \alpha^2 B_2) \frac{\partial v_R}{\partial z} + \alpha\gamma B_2 \frac{\partial v_Z}{\partial r} \\ \mathbf{e}_z \cdot \mathbf{D}^\bullet \cdot \mathbf{e}_\phi &= (\chi_3 + \alpha^2 B_1) \frac{\partial v_\phi}{\partial z} + \frac{\alpha\gamma B_1}{r} \frac{\partial v_Z}{\partial \varphi} \\ \mathbf{e}_z \cdot \mathbf{D}^\bullet \cdot \mathbf{e}_Z &= 2\alpha\gamma \chi_{13} \frac{\partial v_R}{\partial r} + \frac{2\alpha\gamma \chi_{23}}{r} \left(\frac{\partial v_\phi}{\partial \varphi} + v_R \right) + (\chi_3 + 2\gamma^2 \chi_{33}) \frac{\partial v_Z}{\partial z} \end{aligned} \quad (23)$$

Similarly, according to the relations (8)–(10), (19), (20), (22), the components of the linearized surface stress tensors of the Piola type \mathbf{D}_+^\bullet and \mathbf{D}_-^\bullet are written as follows:

$$\begin{aligned}
\mathbf{e}_r \cdot \mathbf{D}_\pm^\bullet \cdot \mathbf{e}_R &= (\kappa_1^\pm + 6\alpha^2\kappa_2^\pm + \xi^\pm) \frac{\partial v_R^\pm}{\partial r} + \frac{\xi^\pm}{r} \left(\frac{\partial v_\Phi^\pm}{\partial \varphi} + v_R^\pm \right) \\
\mathbf{e}_r \cdot \mathbf{D}_\pm^\bullet \cdot \mathbf{e}_\Phi &= (\kappa_1^\pm + 4\alpha^2\kappa_2^\pm) \frac{\partial v_\Phi^\pm}{\partial r} + \frac{2\alpha^2\kappa_2^\pm}{r} \left(\frac{\partial v_R^\pm}{\partial \varphi} - v_\Phi^\pm \right) \\
\mathbf{e}_r \cdot \mathbf{D}_\pm^\bullet \cdot \mathbf{e}_Z &= (\kappa_1^\pm + 2\alpha^2\kappa_2^\pm) \frac{\partial v_Z^\pm}{\partial r} \\
\mathbf{e}_\varphi \cdot \mathbf{D}_\pm^\bullet \cdot \mathbf{e}_R &= 2\alpha^2\kappa_2^\pm \frac{\partial v_\Phi^\pm}{\partial r} + \frac{\kappa_1^\pm + 4\alpha^2\kappa_2^\pm}{r} \left(\frac{\partial v_R^\pm}{\partial \varphi} - v_\Phi^\pm \right) \\
\mathbf{e}_\varphi \cdot \mathbf{D}_\pm^\bullet \cdot \mathbf{e}_\Phi &= \xi^\pm \frac{\partial v_R^\pm}{\partial r} + \frac{\kappa_1^\pm + 6\alpha^2\kappa_2^\pm + \xi^\pm}{r} \left(\frac{\partial v_\Phi^\pm}{\partial \varphi} + v_R^\pm \right) \\
\mathbf{e}_\varphi \cdot \mathbf{D}_\pm^\bullet \cdot \mathbf{e}_Z &= \frac{\kappa_1^\pm + 2\alpha^2\kappa_2^\pm}{r} \frac{\partial v_Z^\pm}{\partial \varphi} \quad \mathbf{e}_z \cdot \mathbf{D}_\pm^\bullet = \mathbf{0}
\end{aligned} \tag{24}$$

$$\xi^\pm = 2\alpha^2(\kappa_{11}^\pm + 4\alpha^2\kappa_{12}^\pm + 4\alpha^4\kappa_{22}^\pm)$$

$$v_R^\pm = v_R|_{z=\pm h}, \quad v_\Phi^\pm = v_\Phi|_{z=\pm h}, \quad v_Z^\pm = v_Z|_{z=\pm h}$$

Taking into account the expressions (23), we write the equations of neutral equilibrium (13), describing the perturbed state of the circular plate, in the scalar form:

$$\begin{aligned}
&(\chi_1 + 2\alpha^2\chi_{11}) \frac{\partial^2 v_R}{\partial r^2} + \frac{\alpha^2(B_3 + 2\chi_{12})}{r} \frac{\partial^2 v_\Phi}{\partial r \partial \varphi} + \alpha\gamma(B_2 + 2\chi_{13}) \frac{\partial^2 v_Z}{\partial r \partial z} \\
&+ \frac{\chi_2 + \alpha^2 B_3}{r^2} \frac{\partial^2 v_R}{\partial \varphi^2} + (\chi_3 + \alpha^2 B_2) \frac{\partial^2 v_R}{\partial z^2} + \frac{\chi_1 + 2\alpha^2 \chi_{11}}{r} \frac{\partial v_R}{\partial r} \\
&- \frac{2\chi_2 + \alpha^2(B_3 + 2\chi_{22})}{r^2} \frac{\partial v_\Phi}{\partial \varphi} - \frac{\chi_2 + 2\alpha^2 \chi_{22}}{r^2} v_R = 0 \\
&(\chi_1 + \alpha^2 B_3) \frac{\partial^2 v_\Phi}{\partial r^2} + \frac{\alpha^2(B_3 + 2\chi_{12})}{r} \frac{\partial^2 v_R}{\partial r \partial \varphi} + \frac{\chi_2 + 2\alpha^2 \chi_{22}}{r^2} \frac{\partial^2 v_\Phi}{\partial \varphi^2} \\
&+ \frac{\alpha\gamma(B_1 + 2\chi_{23})}{r} \frac{\partial^2 v_Z}{\partial \varphi \partial z} + (\chi_3 + \alpha^2 B_1) \frac{\partial^2 v_\Phi}{\partial z^2} + \frac{\chi_1 + \alpha^2 B_3}{r} \frac{\partial v_\Phi}{\partial r} \\
&+ \frac{2\chi_2 + \alpha^2(B_3 + 2\chi_{22})}{r^2} \frac{\partial v_R}{\partial \varphi} - \frac{\chi_2 + \alpha^2 B_3}{r^2} v_\Phi = 0 \\
&(\chi_1 + \gamma^2 B_2) \frac{\partial^2 v_Z}{\partial r^2} + \alpha\gamma(B_2 + 2\chi_{13}) \frac{\partial^2 v_R}{\partial r \partial z} + \frac{\chi_2 + \gamma^2 B_1}{r^2} \frac{\partial^2 v_Z}{\partial \varphi^2} \\
&+ \frac{\alpha\gamma(B_1 + 2\chi_{23})}{r} \frac{\partial^2 v_\Phi}{\partial \varphi \partial z} + (\chi_3 + 2\gamma^2 \chi_{33}) \frac{\partial^2 v_Z}{\partial z^2} \\
&+ \frac{\chi_1 + \gamma^2 B_2}{r} \frac{\partial v_Z}{\partial r} + \frac{\alpha\gamma(B_2 + 2\chi_{23})}{r} \frac{\partial v_R}{\partial z} = 0
\end{aligned} \tag{25}$$

According to the relations (22)–(24), the linearized equilibrium conditions (18) on the plate faces are written as follows ($z = \pm h$):

$$\begin{aligned}
 & \left(\chi_3 + \alpha^2 B_2 \right) \frac{\partial v_R}{\partial z} + \alpha \gamma B_2 \frac{\partial v_Z}{\partial r} \mp (\kappa_1^\pm + 6\alpha^2 \kappa_2^\pm + \xi_\pm) \left(\frac{\partial^2 v_R}{\partial r^2} + \frac{1}{r} \frac{\partial v_R}{\partial r} - \frac{v_R}{r^2} \right) \\
 & \mp \frac{2\alpha^2 \kappa_2^\pm + \xi_\pm}{r} \left(\frac{\partial^2 v_\phi}{\partial r \partial \phi} - \frac{1}{r} \frac{\partial v_\phi}{\partial \phi} \right) \mp \frac{\kappa_1^\pm + 4\alpha^2 \kappa_2^\pm}{r^2} \left(\frac{\partial^2 v_R}{\partial \phi^2} - 2 \frac{\partial v_\phi}{\partial \phi} \right) = 0 \\
 & \left(\chi_3 + \alpha^2 B_1 \right) \frac{\partial v_\phi}{\partial z} + \frac{\alpha \gamma B_1}{r} \frac{\partial v_Z}{\partial \phi} \mp \frac{2\alpha^2 \kappa_2^\pm + \xi_\pm}{r} \left(\frac{\partial^2 v_R}{\partial r \partial \phi} + \frac{1}{r} \frac{\partial^2 v_\phi}{\partial \phi^2} + \frac{1}{r} \frac{\partial v_R}{\partial \phi} \right) \quad (26) \\
 & \mp (\kappa_1^\pm + 4\alpha^2 \kappa_2^\pm) \left(\frac{\partial^2 v_\phi}{\partial r^2} + \frac{1}{r} \frac{\partial v_\phi}{\partial r} - \frac{v_\phi}{r^2} + \frac{1}{r^2} \frac{\partial^2 v_\phi}{\partial \phi^2} + \frac{2}{r^2} \frac{\partial v_R}{\partial \phi} \right) = 0 \\
 & \left(\chi_3 + 2\gamma^2 \chi_{33} \right) \frac{\partial v_Z}{\partial z} + 2\alpha \gamma \chi_{13} \frac{\partial v_R}{\partial r} + \frac{2\alpha \gamma \chi_{23}}{r} \left(\frac{\partial v_\phi}{\partial \phi} + v_R \right) \\
 & \mp (\kappa_1^\pm + 2\alpha^2 \kappa_2^\pm) \left(\frac{\partial^2 v_Z}{\partial r^2} + \frac{1}{r} \frac{\partial v_Z}{\partial r} + \frac{1}{r^2} \frac{\partial^2 v_Z}{\partial \phi^2} \right) = 0
 \end{aligned}$$

while the linearized edge conditions (21) take the form ($r = r_0$):

$$\left(\chi_1 + \gamma^2 B_2 \right) \frac{\partial v_Z}{\partial r} + \alpha \gamma B_2 \frac{\partial v_R}{\partial z} = 0, \quad v_R = 0, \quad v_\phi = 0 \quad (27)$$

Thus, the stability analysis of a circular plate with surface stresses in the general case is reduced to solving a linear homogeneous boundary-value problem (25)–(27) for the system of three partial differential equations.

5 Axisymmetric Buckling

In the special case of axisymmetric perturbations ($\partial v_R / \partial \phi = 0$, $\partial v_\phi / \partial \phi = 0$, $\partial v_Z / \partial \phi = 0$), the boundary-value problem (25)–(27) becomes much simpler. The use of substitution [13]

$$v_R = V_R(z) J_1(\beta r), \quad v_\phi = V_\phi(z) J_1(\beta r) \quad v_Z = V_Z(z) J_0(\beta r) \quad (28)$$

$$\beta = \zeta_m / r_0, \quad J_1(\zeta_m) = 0, \quad m = 1, 2, \dots$$

leads to the separation of the variable r in the problem and allows to satisfy the linearized boundary conditions (27) at the edge of the plate. Here J_0 and J_1 are the Bessel functions of the first kind.

Given the representation (28), the linearized equilibrium equations (25) are written as follows (hereinafter ' denotes the derivative with respect to z):

$$\begin{aligned} (\chi_3 + \alpha^2 B_2) V_R'' - \beta^2 (\chi_1 + 2\alpha^2 \chi_{11}) V_R - \alpha\beta\gamma (B_2 + 2\chi_{13}) V_Z' &= 0 \\ (\chi_3 + \alpha^2 B_1) V_\phi'' - \beta^2 (\chi_1 + \alpha^2 B_3) V_\phi &= 0 \\ (\chi_3 + 2\gamma^2 \chi_{33}) V_Z'' - \beta^2 (\chi_1 + \gamma^2 B_2) V_Z + \alpha\beta\gamma (B_2 + 2\chi_{13}) V_R' &= 0 \end{aligned} \tag{29}$$

Similarly, the linearized equilibrium conditions (26) take the form ($z = \pm h$):

$$\begin{aligned} (\chi_3 + \alpha^2 B_2) V_R' \pm \beta^2 (\kappa_1^\pm + 6\alpha^2 \kappa_2^\pm + \xi_\pm) V_R - \alpha\beta\gamma B_2 V_Z &= 0 \\ (\chi_3 + \alpha^2 B_1) V_\phi' \pm \beta^2 (\kappa_1^\pm + 4\alpha^2 \kappa_2^\pm) V_\phi &= 0 \\ (\chi_3 + 2\gamma^2 \chi_{33}) V_Z' + 2\alpha\beta\gamma \chi_{13} V_R \pm \beta^2 (\kappa_1^\pm + 2\alpha^2 \kappa_2^\pm) V_Z &= 0 \end{aligned} \tag{30}$$

As a result, the axisymmetric buckling analysis for the circular plate with surface stresses is reduced to solving a linear homogeneous boundary-value problem (29), (30) for the system of three ordinary differential equations.

If the elastic properties of the top and bottom faces of the plate are the same, i.e. $\kappa_\theta^+ = \kappa_\theta^-$ and $\kappa_{\theta\tau}^+ = \kappa_{\theta\tau}^-$ ($\theta, \tau = 1, 2$), then the boundary-value problem (29), (30) has two independent sets of solutions [13, 15]. The **First set** is formed by solutions for which the deflection of a plate is an odd function of z (symmetric buckling):

$$V_R(z) = V_R(-z), \quad V_\phi(z) = V_\phi(-z), \quad V_Z(z) = -V_Z(-z)$$

For the **Second set** of solutions, the deflection is an even function of z (flexural buckling):

$$V_R(z) = -V_R(-z), \quad V_\phi(z) = -V_\phi(-z), \quad V_Z(z) = V_Z(-z)$$

Due to this, it is sufficient to consider only half of the plate ($0 \leq z \leq h$) to study its stability. The boundary conditions at the middle surface ($z = 0$) follow from the evenness and oddness of the unknown functions V_R, V_ϕ, V_Z :

a) for the **First set** of solutions:

$$V_R'(0) = V_\phi'(0) = V_Z(0) = 0 \tag{31}$$

b) for the **Second set** of solutions:

$$V_R(0) = V_\phi(0) = V_Z'(0) = 0 \tag{32}$$

Thus, the stability analysis of a plate with identical faces can be reduced to solving two linear homogeneous boundary-value problems for the half-plate: (29)–(31) and (29), (30), (32).

6 Numerical Results

As an example, we have studied the stability of a circular plate made of aluminum in the case of axisymmetric perturbations. Two different models of bulk material were considered:

1) Harmonic model [7] ($\lambda_1, \lambda_2, \lambda_3$ are the principal stretches)

$$W = \frac{1}{2}\lambda (\lambda_1 + \lambda_2 + \lambda_3 - 3)^2 + 2\mu [(\lambda_1 - 1)^2 + (\lambda_2 - 1)^2 + (\lambda_3 - 1)^2]$$

$$\lambda_k = \sqrt{G_k}, \quad k = 1, 2, 3$$

2) Blatz–Ko model [2] (I_1, I_2, I_3 are the principal invariants of the Cauchy–Green strain tensor)

$$W = \frac{1}{2}\mu b \left(I_1 + \frac{I_3^{-a} - 1}{a} - 3 \right) + \frac{1}{2}\mu (1 - b) \left(\frac{I_2}{I_3} + \frac{I_3^a - 1}{a} - 3 \right), \quad a = \frac{\lambda}{2\mu}$$

$$I_1 = G_1 + G_2 + G_3, \quad I_2 = G_1G_2 + G_1G_3 + G_2G_3, \quad I_3 = G_1G_2G_3$$

The surface strain energy densities were assumed to be quadratic functions of the invariants j_1^\pm, j_2^\pm [1]:

$$W_\pm = \frac{1}{8}\lambda_\pm (j_1^\pm - 2)^2 + \frac{1}{4}\mu_\pm (j_2^\pm - 2j_1^\pm + 2)$$

The following values of bulk λ, μ and surface λ_\pm, μ_\pm elastic moduli were used for the aluminum [4]:

$$\lambda = 52.05 \text{ GPa}, \quad \mu = 34.7 \text{ GPa}, \quad \lambda_\pm = -3.49 \text{ Pa} \cdot \text{m}, \quad \mu_\pm = 6.22 \text{ Pa} \cdot \text{m}$$

For convenience, the following dimensionless parameters were introduced:

- relative radial compression $\delta = 1 - \alpha$,
- radius-to-thickness ratio $r_0^* = r_0/2h$,
- relative thickness $H^* = 2h\mu/\mu_+$.

By numerical solution of the linearized boundary-value problems (29)–(31) and (29), (30), (32) we found the spectra of critical values of the relative radial compression δ , corresponding to the different buckling modes of the circular plate with surface stresses. By analyzing these spectra, the critical radial compression δ_c was obtained for plates of various sizes. It should be noted that we did not study the stability of very thick plates ($r_0^* < 5$) in this paper. As a result, it was determined that the flexural buckling occurs at the lowest loads, and the critical radial compression δ_c corresponds to the first flexural mode ($m = 1$).

Fig. 1 Size effect on the stability of circular plate with surface stresses. Harmonic model

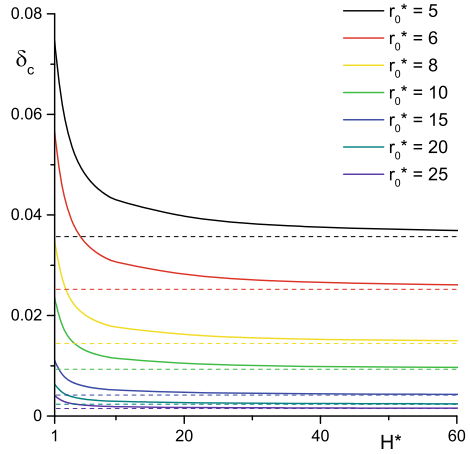
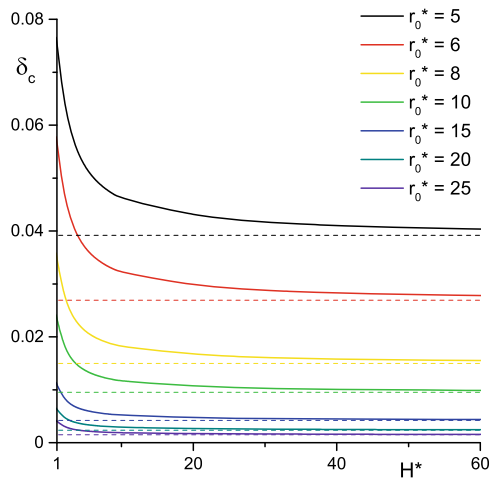


Fig. 2 Size effect on the stability of circular plate with surface stresses. Blatz–Ko model ($b = 0$)



Figures 1 and 2 illustrate the influence of the overall size (scale) of the plate on its stability. The graphs show the dependencies (solid lines) of the critical radial compression δ_c on the relative thickness H^* (size parameter) for plates with the different radius-to-thickness ratio r_0^* . According to the results obtained for both models of bulk material, the stability of the plate increases with a decrease in size. This effect is due to the influence of surface stresses. It is negligible at the macroscale but becomes quite significant at micro- and nanoscale ($H^* \leq 50$). For reference, the graphs also show the results of the stability analysis for plates without surface stresses (dashed lines). As expected, these results do not depend on the overall size of the plate.

Additionally, we have analyzed how the geometric proportions (ratios of linear dimensions) of the circular plate affect its stability. The results are reflected in Figs. 3

Fig. 3 Effect of plate proportions on its stability. Harmonic model

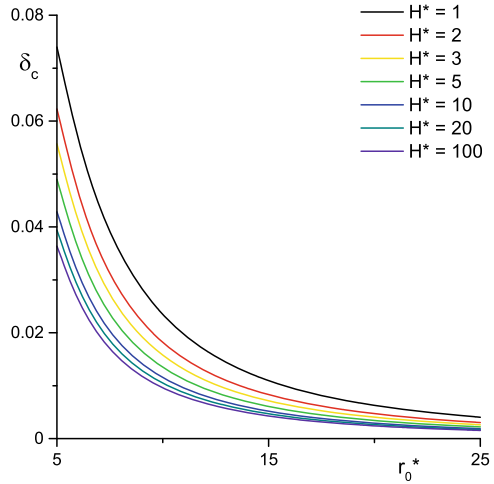
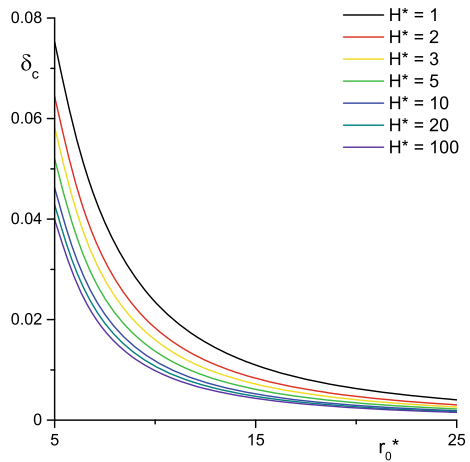


Fig. 4 Effect of plate proportions on its stability. Blatz–Ko model ($b = 0$)



and 4 which show the dependencies of the critical radial compression δ_c on the radius-to-thickness ratio r_0^* for plates of different scale H^* . According to them, the thicker plates are generally more stable, and this fact is more pronounced for smaller plates due to the influence of surface stresses.

7 Conclusion

In the framework of the bifurcation approach, we studied the stability of a nonlinearly elastic circular plate with surface stresses. For an arbitrary isotropic material, the system of linearized equilibrium equations was derived, which describes the behavior

of a plate in a perturbed state. In the case of axisymmetric perturbations, the stability analysis was reduced to solving a linear homogeneous boundary-value problem (29), (30) for a system of three ordinary differential equations. Additionally, it was established that if the elastic properties of the top and bottom faces of the plate are the same, then it is sufficient to consider only half of the plate to study its stability. For two specific models of bulk material (Harmonic model and Blatz–Ko model), the buckling analysis has been carried out for a circular plate made of aluminum in the case of axisymmetric perturbations. As a result, it was found that the stability of the plate increases with a decrease in its overall size. This effect is due to the influence of surface stresses. It is negligible at the macroscale but becomes quite significant at micro- and nanoscale ($H^* \leq 50$).

Acknowledgements This work was supported by the Russian Foundation for Basic Research (grants 16-08-00802-a, 16-01-00647-a, 16-48-230068-r_a) and by the Ministry of Science and Higher Education of the Russian Federation (Project 01201354242).

References

1. Altenbach, H., Morozov, N.F. (eds.): *Surface Effects in Solid Mechanics—Models, Simulations, and Applications*. Springer, Berlin (2013)
2. Blatz, P.J., Ko, W.L.: Application of finite elastic theory to the deformation of rubbery materials. *Trans. Soc. Rheology* **6**, 223–251 (1962)
3. Cuenot, S., Fretigny, C., Demoustier-Champagne, S., Nysten, B.: Surface tension effect on the mechanical properties of nanomaterials measured by atomic force microscopy. *Phys. Rev. B* **69**(16), 165, 410–415 (2004)
4. Duan, H.L., Wang, J., Karihaloo, B.L.: Theory of elasticity at the nanoscale. In: *Advances in Applied Mechanics*, vol. 42, pp. 1–68. Elsevier, San Diego (2008)
5. Green, A.E., Adkins, J.E.: *Large Elastic Deformations and Non-Linear Continuum Mechanics*. Clarendon Press, Oxford (1960)
6. Gurtin, M.E., Murdoch, A.I.: A continuum theory of elastic material surfaces. *Arch. Ration. Mech. Anal.* **57**(4), 291–323 (1975)
7. John, F.: Plane strain problems for a perfectly elastic material of harmonic type. *Commun. Pure Appl. Math.* **13**, 239–296 (1960)
8. Lurie, A.I.: *Non-linear Theory of Elasticity*. North-Holland, Amsterdam (1990)
9. Miller, R.E., Shenoy, V.B.: Size-dependent elastic properties of nanosized structural elements. *Nanotechnology* **11**(3), 139–147 (2000)
10. Ogden, R.W.: *Non-Linear Elastic Deformations*. Dover, Mineola (1997)
11. Ogden, R.W., Steigmann, D.J., Haughton, D.M.: The effect of elastic surface coating on the finite deformation and bifurcation of a pressurized circular annulus. *J. Elast.* **47**(2), 121–145 (1997)
12. Sheyidakov, D.N.: Stability of a rectangular plate under biaxial tension. *J. Appl. Mech. Tech. Phy.* **48**(4), 547–555 (2007)
13. Sheyidakov, D.N.: Size effect on buckling of non-uniform circular plate made of foam material. *Mater. Phys. Mech.* **28**(1–2), 26–30 (2016)
14. Sheyidakov, D.N.: Effect of surface stresses on stability of elastic circular cylinder. In: dell’Isola, F., Eremeyev, V., Porubov, A. (eds.) *Advances in Mechanics of Microstructured Media and Structures, Advanced Structured Materials*, vol. 87, pp. 343–355. Springer, Cham (2018)
15. Sheyidakov, D.N.: On stability of a nonlinearly elastic rectangular plate with surface stresses. In: Pietraszkiewicz, W., Witkowski, W. (eds.) *Shell Structures: Theory and Applications*, vol. 4, pp. 271–274. CRC Press, London (2018)

16. Wang, J., Duan, H.L., Huang, Z.P., Karihaloo, B.L.: A scaling law for properties of nanostructured materials. *P. Roy. Soc. Lond. A* **462**(2069), 1355–1363 (2006)
17. Wang, J., Huang, Z., Duan, H., Yu, S., Feng, X., Wang, G., Zhang, W., Wang, T.: Surface stress effect in mechanics of nanostructured materials. *Acta Mech. Solida. Sin.* **24**, 52–82 (2011)
18. Zubov, L.M.: *Nonlinear Theory of Dislocations and Disclinations in Elastic Bodies*. Springer, Berlin (1997)